ANNALES
UNIVERSITATIS MARIAE CURIE-SKŁODOWSKA
LUBLIN - POLONIA
VOL. L/LI SECTIO AAA 1995/1996

Institute of Physics, M. Curie-Skłodowska University,
20-031 Lublin, pl. M. Curie-Skłodowskiej 1, Poland

ZDZISŁAW ŁOJEWSKI, ANDRZEJ STASZCZAK

Spontaneous Fission Half-Lives of the Heaviest Nuclei Calculated with Woods-Saxon Potential

Czasy połowicznego zaniku najcięższych jąder atomowych w procesie spontanicznego rozszczepienia obliczone z uwzględnieniem potencjału Woodsa-Saxona

1. INTRODUCTION

In the seventies many theoretical calculations of the spontaneous fission half-lives T_{sf} were done. Those calculations have been based mainly on the Nilsson single particle potential [1] and the static [2–4] or the dynamic approximation [5–7]. A successful description of the spontaneous fission half-lives T_{sf} of experimentally known heaviest nuclei and the prediction of existence of the shape isomers were essential achievements of those investigations.

In particular, the theoretical model predicted well the T_{sf} of the fermium and nobelium isotopes [5, 7], e.g. a very fast decrease of the spontaneous fission half-lives with an increasing number of neutrons ($N > 152$). But for the nuclei heavier than Z = 102, the agreement between experiment and theoretical estimates were essentially worse. Especially the T_{sf} of the heaviest nuclei ($Z = 108, 110$) appeared to be too small.

It was a reason to search for a better theoretical description of these properties. A proper choice of the single-particle nuclear potential is of fundamental importance for a wide variety of nuclear calculations.

The papers [8, 9] on the spontaneous fission and alpha decay half-lives have been based on another, more realistic single particle model: the Woods-Saxon potential [10]. The calculations were done for even-even [8] and odd-A and odd-odd [9] nuclei with atomic number $Z \geqslant 104$ in static approximation and with the phenomenological effective inertia only. Their promising results which agree with the experimental data for Z=104 isotopes were good stimulation to extend these calculations.

In recent years a number of theoretical papers have been devoted to estimate the properties of the heaviest nuclei with Woods-Saxon potential. In the paper [11] the two fission modes (static paths to fission) of the heavy fermium isotopes (so-called "bimodal" fission) were explained. The model used in this paper has been based on the Woods-Saxon potential in the multidimensional deformation space (β_λ, $\lambda = 2 \div 9$) and Strutinsky [12, 1] shell correction method.

In the paper [13] the ground state properties of the heaviest nuclei ($Z = 90 \div 114$) were analyzed in the three-dimensional deformation space (β_λ, $\lambda = 2, 4, 6$). It was found there that the use of the larger deformation space significantly improves the description of the experimental data.

The paper [14] on the potential energy and fission barriers of superheavy nuclei predicted the fission lifetimes of nuclei with $Z = 112 \div 130$ in statical model and with the phenomenological mass parameter. The authors have shown that the fission lifetimes are larger than the alpha-decay half-lives for most of the considered nuclides. In the paper [15] the authors give information about the shell structure, equilibrium deformations and binding energies of nuclei with atomic number $Z = 95 \div 111$.

The paper [16] on the spontaneous fission half-lives gives T_{sf} in dynamical approximation of the even-even nuclei with proton number $Z \geqslant 104$, for which the fission barriers are relatively simple and thin. The dynamical calculations of T_{sf} have been done in the two-dimensional deformation space (β_2, β_4) with the simultaneous minimization of the potential energy V in the remaining degrees of freedom (β_3, β_5, β_6 andβ_8) and with the full mass tensor B in the adequate points. But as we demonstrate a detailed study of the T_{sf} in deformation spaces of various dimensions has shown that this "combined" approximation is not good for lighter nuclei($Z \sim 100$) considered in the present paper. Therefore, in this paper we will consequently use only the full dynamical method. To minimize the action integral we have applied the dynamic-programming method [5].

In the present study we use a 4-dimensional collective space ($\beta_2, \beta_4, \Delta_p$, Δ_n). Except the shape deformations β_2 and β_4, describing the elongation and neck of nuclei we add the pairing protons and neutrons gaps Δ_p and

Δ_n as new collective coordinates. It was done in order to get the coupling of the shape and pairing vibrations. The earlier microscopic calculations [17], in 3-dimensional $(\beta_{24}, \Delta_p, \Delta_n)$ model and with Nilsson potential show that this effect plays the important role in the estimation of the fission lifetime.

In order to examine the above effects we extended the dynamic programming method up to four collective degrees of freedom; the calculations in more-dimensional collective space are practically impossible. The present paper is a continuation of our previous research [9] in which a theoretical estimate of the half-lives T_{sf} with Woods-Saxon potential has been obtained. We concentrate on the even-even nuclei with the atomic number Z=100–110. The half-lives T_{sf} are calculated both in the static and the dynamic approach.

The main differences with respect to the previous papers are:

- the full dynamical method of calculations of T_{sf} (the static T_{sf} are given only for comparison);
- extension of the dynamic-programming method up to four collective degrees of freedom;
- inclusion of the pairing degrees of freedom (Δ_p and Δ_n), describing the coupling of the collective pairing vibrations with the fission mode;
- usage of the full microscopic adiabatic cranking model for mass tensor B instead of the phenomenological formulae.

The method of evaluation of the T_{sf} is described in Sect. 2. In Sect. 3 the main results are presented. Conclusions are drawn in Sect. 4.

2. THEORETICAL MODEL

We have used the single-particle deformed Woods-Saxon potential. As this potential is widely described in the literature (see e.g. [10, 18]), we restricted ourselves to a brief presentation of the basic formulae only.

The Woods-Saxon potential consists of the central part V_{cent}, the spin-orbit term V_{so} and the Coulomb potential V_{Coul} for protons:

$$V^{WS}(\vec{r}, \vec{p}, \vec{s}; \beta) = V_{\text{cent}}(\vec{r}; \beta) + V_{so}(\vec{r}, \vec{p}, \vec{s}; \beta) + V_{\text{Coul}}(\vec{r}; \beta) \tag{1}$$

The central part is defined by

$$V_{\text{cent}}(\vec{r}; \beta) = \frac{V_0[1 \pm \kappa(N-Z)/(N+Z)]}{[1 + exp(l(\vec{r}; \beta)/a)]}, \tag{2}$$

where parameter a describes the diffuseness of the nuclear surface, the plus (+) sign holding for protons, the minus (−) sign for neutrons and $\kappa = 0.86$ [18]. The set of β_λ parameters is denoted by β. The function $l(\vec{r}, \beta)$, describing the distance between a given point $\vec{r}$ and the nuclear surface has been determined numerically [10].

The spin orbit potential was taken as

$$V_{so}(\vec{r}, \vec{p}, \vec{s}; \beta) = -\lambda(\nabla V_{\text{cent}} \times \vec{p}) \cdot \vec{s}. \tag{3}$$

The Coulomb potential for protons is assumed to be that of the uniform charge distribution with sharp edges. In our calculations we have used the single-particle W-S potential with the "universal" set of its parameters adjusted to the single-particle levels of all odd-A nuclei with $A \geqslant 40$. The values of the 12 constants which determine the W-S potential parametrisation are specified in Ref. [18].

According to the Strutinsky model [12], the collective potential energy surface reads

$$V(q) = E_{\text{macr}}(q) + \delta E_{\text{shell}}(q) + \delta E_{\text{pair}}(q)\,. \tag{4}$$

Here $E_{\text{macr}}(q)$ is the macroscopic, smooth part energy. The argument "q" denotes the set of collective variables used in our calculations $q = (\beta_2, \beta_4, \Delta_p, \Delta_n)$. Other two terms correspond to the shell correction δE_{shell} and the pairing correction δE_{pair}. The details of the smoothing procedure when evaluating δE_{shell} and the calculations of δE_{pair} are completely analogous to those described in Refs. [2–9].

Two models for the smooth part of the energy E_{macr}, entering the formula (4) were applied. One is the liquid drop model [19] and the second one is the folded Yukawa plus exponential term [20, 21].

We include the pairing forces in BCS scheme with constant matrix element of interaction G independent of deformation:

$$\bar{\mathcal{H}}_{BCS} = -G \sum_{a,a'} \bar{P}_a^+ \bar{P}_{a'}\,, \tag{5}$$

where $\bar{P}_a^+$ and $\bar{P}_a$ are the creation and annihilation operators of the pair of particles conjugate to zero angular momentum: $|a\rangle \sim |\nu\bar{\nu}\rangle$ and $|\nu\rangle$ and $|\bar{\nu}\rangle$ are the time reversed conjugate single particle states.

In the whole calculation we have used the pairing strength constants as follows [22]: for protons $G_Z A = 13.3 + 0.217(N - Z)$ and for neutrons $G_N A = 19.3 - 0.084(N - Z)$, where N, Z and A are proton, neutron and mass number $A = N + Z$ respectively. The number of levels in the pairing

window equals to the number of particles (Z or N) and is counted from the bottom of the energy spectrum.

In the adiabatic cranking model the collective mass $B_{kl}(q)$ reads

$$B_{kl}(q) = 2\hbar^2 \sum_{m\neq 0} \frac{\langle m|\frac{\partial \mathcal{H}}{\partial q_k}|0\rangle\langle 0|\frac{\partial \mathcal{H}}{\partial q_l}|m\rangle}{(\varepsilon_m - \varepsilon_0)^3}, \tag{6}$$

where $|m\rangle$ and $|0\rangle$ denote the wave function of the excited and ground state of the nucleus, respectively; ε_m and ε_0 are the corresponding energies.

After transforming to the quasi-particle representation and calculating of the derivative of the collective Hamiltonian $\mathcal{H}$ over the variables q_k, the formulae takes the following form:

$$B_{kl}(q) = 2\hbar^2 \sum_{\mu,\nu} (P_k)_{\mu\nu}(E_\nu + E_\mu)^{-1}(P_l)_{\mu\nu} \tag{7}$$

where

$$(P_k)_{\mu\nu}(\beta_i) = -\frac{\langle \mu|\frac{\partial H_s}{\partial \beta_k}|\nu\rangle}{E_\mu + E\nu}(u_\mu v_\nu + u_\nu v_\mu) - \delta_{\mu\nu}\left(\frac{\Delta}{E_\mu^2}\frac{\partial \lambda}{\partial \beta_k} - \frac{\lambda}{E_\mu^2}\frac{\partial \Delta}{\partial \beta_k}\right) \tag{8}$$

for shape deformations and

$$(P_k)_{\mu\nu}(\Delta) = \delta_{\mu\nu}\frac{(e_\nu - \lambda) + \Delta\frac{\partial \lambda}{\partial \Delta}}{2E_\nu} \tag{9}$$

for pairing degrees of freedom. Here Δ and λ are the gap energy and Fermi level of nuclei, v_μ, u_μ are the pairing occupation probability factors, the H_s is the single particle Hamiltonian and the E_μ is the quasi-particle energy corresponding to $|\mu\rangle$ state.

We describe the fission process of a nucleus as a tunnelling through the collective potential energy barrier. Using the classical WKB approximation the probability of tunneling reads

$$P = (1 + \mathrm{e}^S)^{-1}, \tag{10}$$

where

$$S = \frac{2}{\hbar}\int_{s_1}^{s_2} \sqrt{2[V(s) - E_{fiss}]\, B_{eff}(s)}\, ds. \tag{11}$$

Here $V(s)$ is the collective potential energy of fissioning nucleus and $B(s)$ is the effective collective inertia. Both collective functions correspond to

a motion along the fission path L(s). The integral limits s_1 and s_2 are the entrance and exit points, respectively. The value of $S/2$ is the reduced Maupertuis action for the "motion" under the potential energy barrier.

The time T_{sf} corresponds to the time in which the half of the number of fissioning nuclei disintegrated. It is inversely proportional to the tunnelling probability

$$T_{sf} = \frac{\ln 2}{n} \frac{1}{P}. \tag{12}$$

In this formula n is the number of assaults of the nucleus on the fission barrier in the time unit. This is frequently calculated from the zero point energy E_{fiss} (for the quadrupole axial vibrations) which in turn is assumed to be the same for all considered nuclei and is equal to 0.5 MeV. This value corresponds to

$$n = \frac{\omega}{2\pi} = \frac{\hbar\omega}{2\pi\hbar} = \frac{0.5\mathrm{MeV\,c}}{\pi c\hbar} \approx \frac{10^{20.38}}{s} \tag{13}$$

assaults.

3. RESULTS

We have used the four-dimensional collective space in the calculations: the deformations β_2 and β_4 describing the elongation and neck of nucleus and the pairing gaps Δ_p and Δ_n, describing the pairing collective degrees of freedom. The potential energy $V(\beta_2, \beta_4, \Delta_p, \Delta_n)$ and ten components of the mass tensor $B_{\mu,\nu}(\beta_2, \beta_4, \Delta_p, \Delta_n)$, where $\mu, \nu = \beta_2, \beta_4, \Delta_p, \Delta_n$, were calculated microscopically in the following grid points:

$$\begin{aligned}
\beta_2 &= \ \ 0.15(0.05)1.40 \quad (26 \text{ points});\\
\beta_4 &= -0.08(0.04)0.40 \quad (13 \text{ points});\\
\Delta_p &= \ \ 0.40(0.20)1.80 \quad (\ 8 \text{ points});\\
\Delta_n &= \ \ 0.40(0.20)1.80 \quad (\ 8 \text{ points}).
\end{aligned}$$

The spontaneous fission half-lives were calculated in the static and the dynamic approach. The static value of the action integral $S(L_{stat})$ was obtained along the fission trajectory minimizing the potential energy only. In the dynamic approach the minimal value of $S(L_{dyn})$ was calculated by minimization of the action integral with respect to all possible trajectories in our 4-dimensional collective space $(\beta_2, \beta_4, \Delta_p, \Delta_n)$.

For illustration a general view of the potential energy surface and three components of the mass tensor $B_{\beta_2\beta_2}$, $B_{\beta_2\beta_4}$, $B_{\Delta_p\Delta_p}$ is shown in Figure 1 for ^{254}Fm nucleus. At each grid point on the maps (β_2, β_4) the energy is

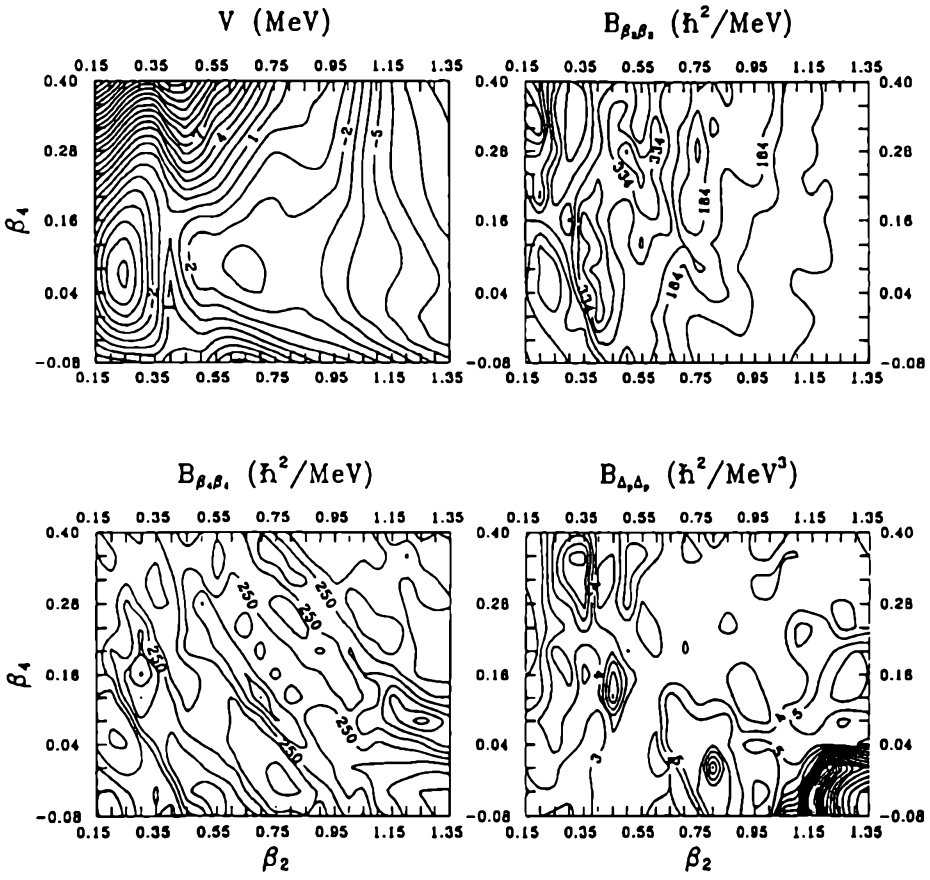

Fig. 1. Potential energy surface and $B_{\beta_2\beta_2}$, $B_{\beta_2\beta_4}$, $B_{\Delta_p\Delta_n}$ components of the mass parameters tensor
Powierzchnie energii potencjalnej i składowych $B_{\beta_2\beta_2}$, $B_{\beta_2\beta_4}$, $B_{\Delta_p\Delta_n}$ tensora parametrów masowych

minimized versus Δ_p and Δ_n degrees of freedom. Figure 1 also illustrates the range of the deformation parameters (β_2 and β_4) considered in the present study.

In order to examine the role of the pairing degrees of freedom we have done the additional calculations in the 2-dimensional deformation space (β_2, β_4). The results are illustrated in the Figure 2 for the fermium isotopes. In the Figure we show the spontaneous fission half-lives T_{sf} in 4-dimensional collective space ($\beta_2, \beta_4, \Delta_p, \Delta_n$) (denoted by square) and in 2-dimensional

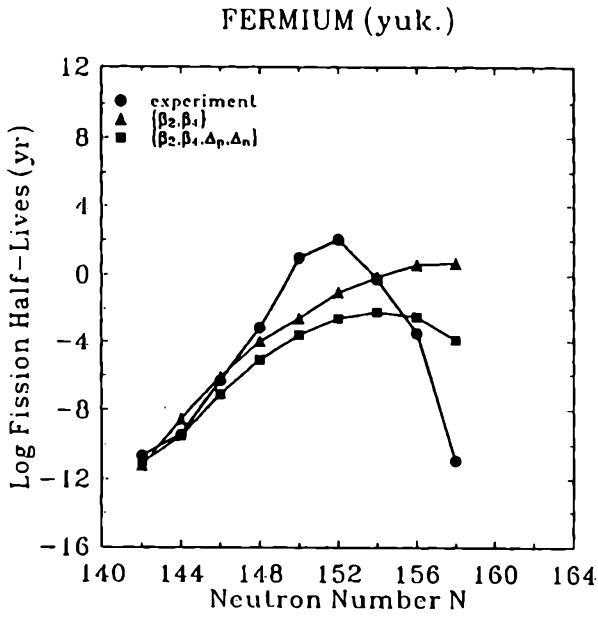

Fig. 2. Spontaneous fission half-lives of the fermium isotopes in $(\beta_2, \beta_4, \Delta_p, \Delta_n)$ and (β_2, β_4) collective spaces

Czasy życia ze względu na proces spontanicznego rozszczepienia izotopów fermu wyznaczone w przestrzeni kolektywnej: $(\beta_2, \beta_4, \Delta_p, \Delta_n)$ oraz (β_2, β_4)

(β_2, β_4) (denoted by up-triangle). For comparison, the experimental data are drawn by means of circles. The difference between the dynamical results of T_{sf} in 4-dimensional space (with Δ_p and Δ_n as collective degrees of freedom) and 2-dimensional space (where the proton and neutron pairing gaps are obtained in the BCS approximation), represents the dynamical effect of the pairing degrees of freedom in our model:

$$\delta T_{sf}(\Delta_p, \Delta_n) = |T_{sf}(\beta_2, \beta_4, \Delta_p, \Delta_n) - T_{sf}(\beta_2, \beta_4)| \,. \tag{14}$$

As it is seen the effect of the pairing degrees of freedom is very strongly isotopic dependent. For lighter isotopes the $\delta T_{sf}(\Delta_p, \Delta_n)$ is about 0.5–1.0 order of magnitude and increase to 4–5 orders of magnitude for heavier Fm isotopes. This effect has been defined similarly in [17] but as a difference between statical values of T_{sf}. Although, as we show further, the statical values of T_{sf} are too big in comparison with experimental data and strongly dependent on the dimensionless of the collective space we apply the δT_{sf}, calculated from dynamical model.

The investigations show that the pairing degrees of freedom are very important in calculations of the spontaneous fission lifetime therefore the

further investigations in this paper are done in 4-dimensional (β_2,β_4,Δ_p,Δ_n) space. For illustration in Figure 3 we show for ^{254}Fm the values of Δ_p and Δ_n through the path to fission in the BCS approximation (dashed line) and in dynamical approach i.e. when pairing degrees of freedom are included (solid line). We can see that the pairing gaps along path to fission in dynamical case are larger about 0.2–0.3 MeV in comparing with statical BCS approximation.

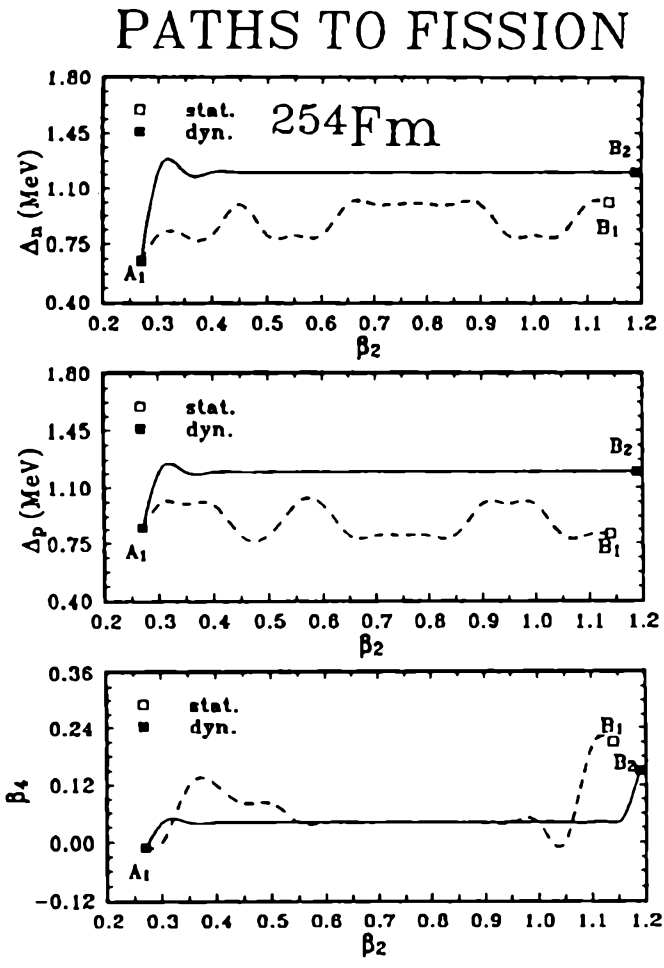

Fig. 3. The dynamical and statical paths to fission in collective space ($\beta_2, \beta_4, \Delta_p, \Delta_n$) for ^{254}Fm

Dynamiczne i statyczne ścieżki do rozszczepienia uzyskane w przestrzeni kolektywnej ($\beta_2, \beta_4, \Delta_p, \Delta_n$) dla ^{254}Fm

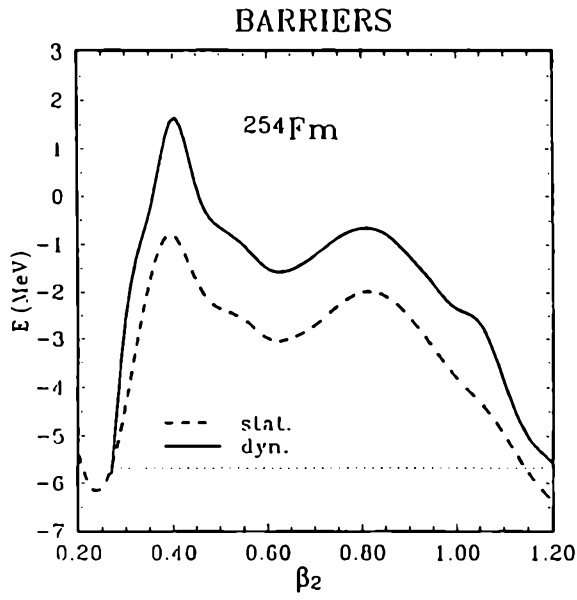

Fig. 4. The dynamical and statical fission barrier for ^{254}Fm
Dynamiczna i statyczna bariera do rozszczepienia dla ^{254}Fm

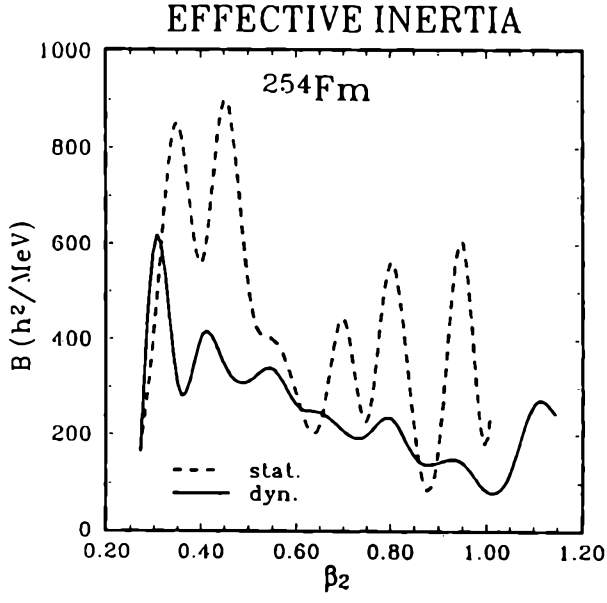

Fig. 5. The dynamical and statical effective mass parameter for ^{254}Fm
Dynamiczny i statyczny efektywny parametr masowy dla ^{254}Fm

Figures 4 and 5 demonstrate the fission barriers and the effective mass parameters along those both (static and dynamic) paths to fission. One can see that the dynamic approach gives larger values of the potential energy V and considerably smaller effective mass parameter B_{eff}.

Spontaneous fission half-lives for the heaviest even-even nuclei with atomic number $Z = 100 \div 110$ are shown in Figures 6–11. In the figures, the results of T_{sf} obtained with the static approach are denoted with a triangle, the results of the dynamic calculations with a square and the experimental values with a circle. Logarithm fission half-lives are given in years. The right part of each figure corresponds to the calculations with folded Yukawa with exponential model [20, 21] and the left with the liquid drop model [19].

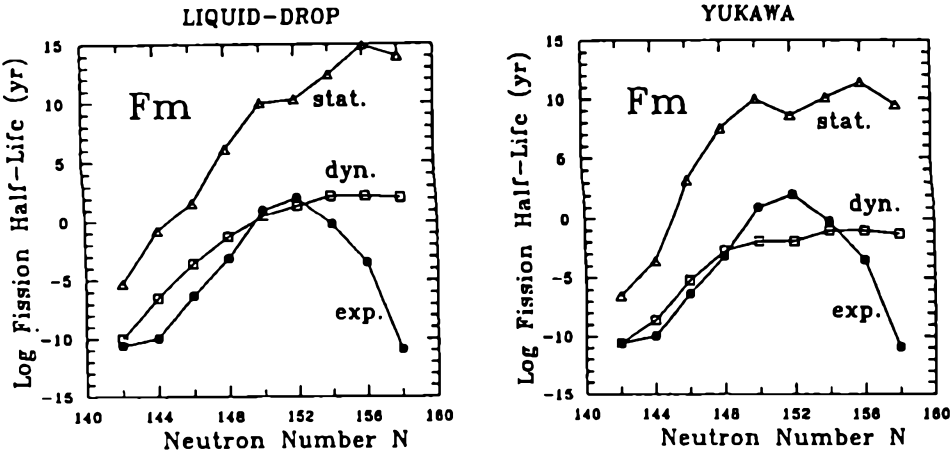

Fig. 6. Spontaneous fission half-lives for fermium isotopes
Czasy życia ze względu na proces spontanicznego rozszczepienia izotopów fermu

The differences between static (triangle) and dynamic (square) estimates of the fission lifetimes increase from 2–4 orders of magnitude for light isotopes to 8–10 orders of magnitude for the heaviest ones. The static estimates are too big in comparison with the experimental data. On the contrary to the earlier papers [8, 9] in which also the Woods-Saxon potential was used we can see that only the dynamical calculations may reproduce the experimental data. For nuclei with atomic numbers Z = 104 and 106 the discrepancies between the results obtained with dynamic model and the experimental values of T_{sf} are not larger than one order of magnitude. It is worthwhile to mention that there are only six experimental points for these nuclei, therefore the good agreement between the theoretical and experimental data is probably accidental.

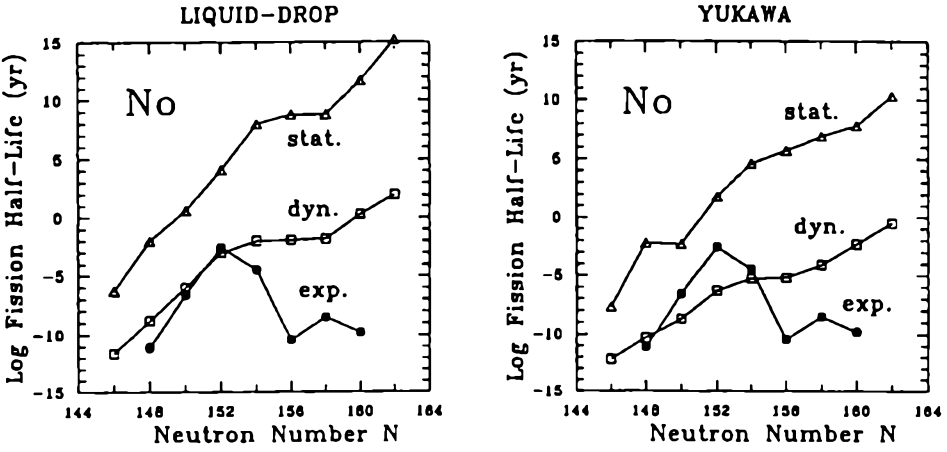

Fig. 7. The same as in Fig. 6 for nobelium isotopes
To samo, co na rycinie 6, lecz dla izotopów noblu

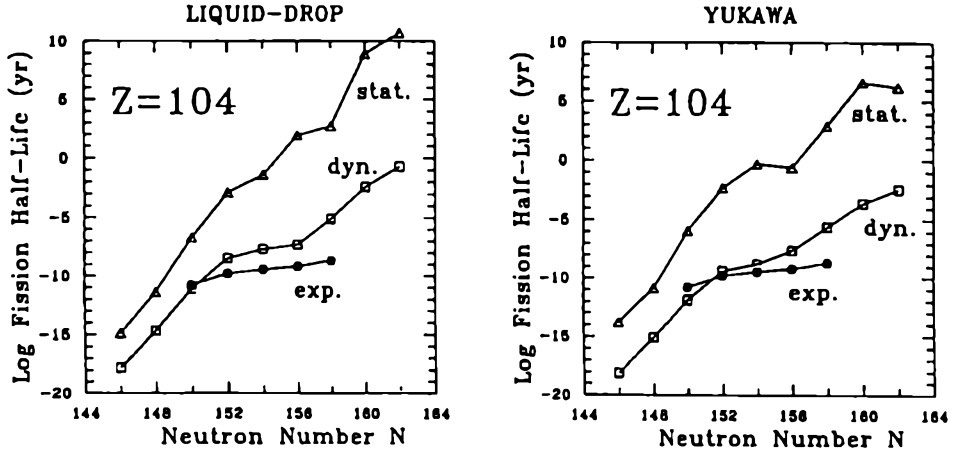

Fig. 8. The same as in Fig. 6 for rutherfordium isotopes
To samo, co na rycinie 6, lecz dla izotopów ruterfordu

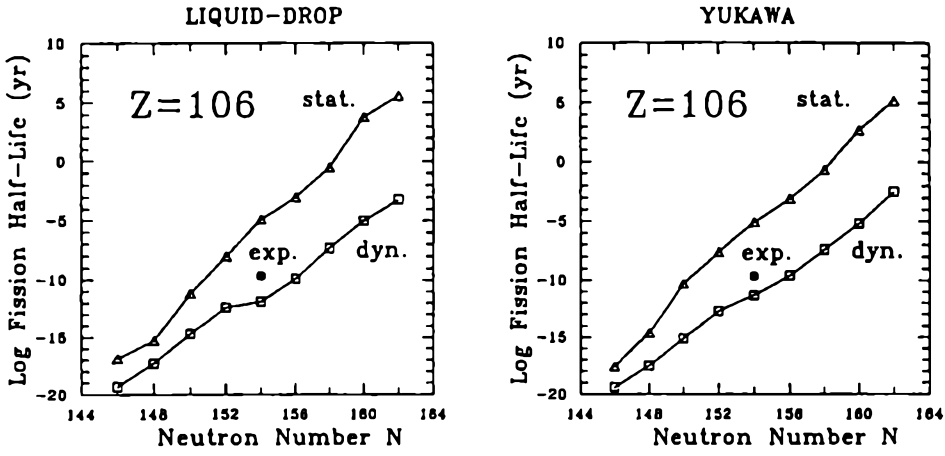

Fig. 9. The same as in Fig. 6 for seaborgium isotopes
To samo, co na rycinie 6, lecz dla izotopów siborgu

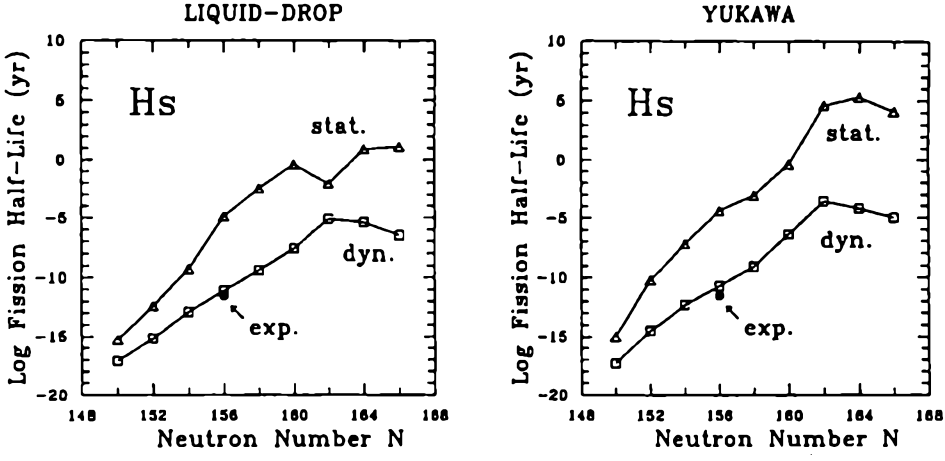

Fig. 10. The same as in Fig. 6 for hassium isotopes
To samo, co na rycinie 6, lecz dla izotopów hassu

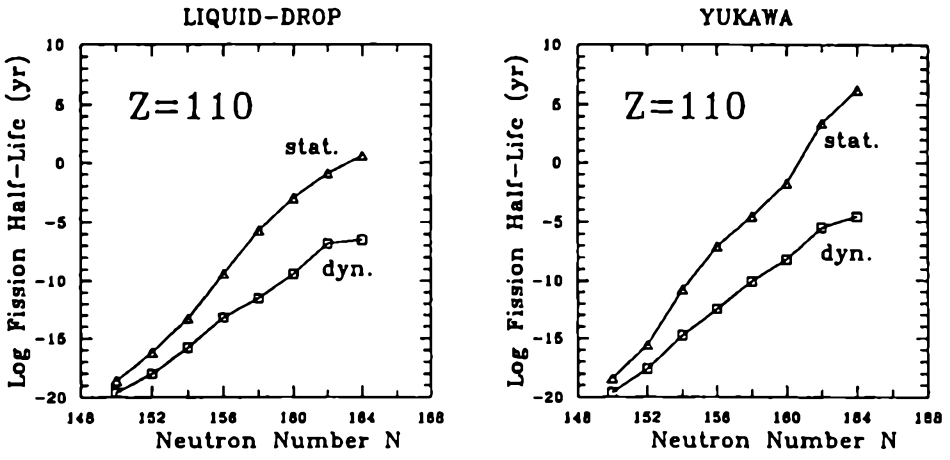

Fig. 11. The same as in Fig. 6 for Z=110 isotopes
To samo, co na rycinie 6, lecz dla izotopów Z=110

A different situation is for the fermium and nobelium isotopes. In the figures we can see that for the lighter isotopes the theoretical and experimental values of T_{sf} are in relatively good agreement. But for the heavier isotopes ($N \geqslant 154$) the agreement is rather poor. In particular we do not observe the well known effect of decrease of the fission lifetimes for heavier isotopes with increase of the neutron numbers. The calculated T_{sf} nearly increases monotonically with N.

It is well known that in the calculations of the fission lifetime the peculiarities of fission barrier play an essential role (height and positions of entrance and exit points, thickness of the barrier). Figure 12 presents the fission barriers of the fermium isotopes as a function of β_2 deformations along the static trajectory, determined by minimizing energy of nuclei by β_4, Δ_p and Δ_n degrees of freedom. Curves are labelled with respective neutron numbers. The left-hand scale corresponds to the lightest isotope (the bottom curve). Other curves are shifted upwards by 2 MeV, subsequently. The results presented in the figure show that the fission barrier heights first increase with neutron number N and next for $N \geqslant 152$ decrease with neutron number. The thickness of the barriers nearly monotonically increase with N. It explains why the theoretical estimates of T_{sf} for fermium isotopes monotonically increase too.

This bad tendency is similar when using the different prescriptions for the smooth part of energy: the folded Yukawa plus exponential or the liquid drop model. So we can draw the conclusion that the increase of the

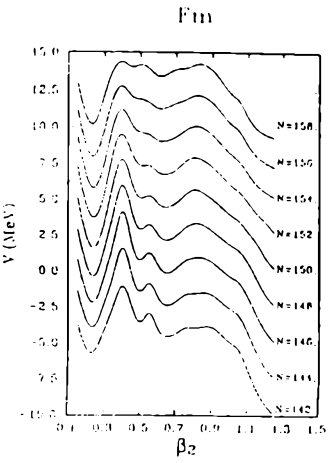

Fig. 12. The fission barriers of the fermium isotopes. The left-hand scale corresponds to the bottom curve. Other curves are shifted upwards by 2 MeV
Bariery na rozszczepienie izotopów fermu. Skala z lewej strony odnosi się do najniższej bariery. Pozostałe bariery przesunięte zostały odpowiednio o 2 MeV do góry każda

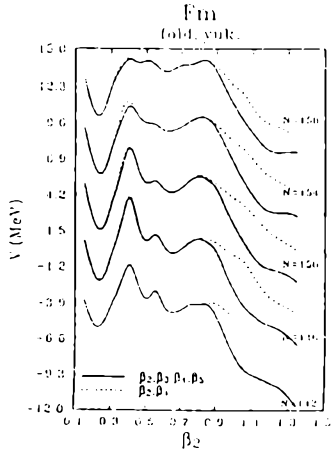

Fig. 13. The fission barriers for the fermium isotopes in $(\beta_2, \beta_3, \beta_4, \beta_5)$ and (β_2, β_4) deformation spaces
Bariery na rozszczepienie izotopów fermu uzyskane w przestrzeni kolektywnej: $(\beta_2, \beta_3, \beta_4, \beta_5)$ i (β_2, β_4)

theoretical T_{sf} with N is connected rather with the poor shell corrections energy determined from Woods-Saxon potential.

In order to improve the strange results of T_{sf} for Fm and No isotopes we have analyzed the dependence of the fission barrier on higher order of deformations.

Since the calculations taking into account the higher order of deformations require much computer time, we restrict ourself to the four dimensional spaces: $(\beta_2, \beta_3, \beta_4, \beta_5)$, describing also the reflection asymmetry shapes of the nucleus and $(\beta_2, \beta_4, \beta_6, \beta_8)$ describing the shapes of nuclei with higher even-multipolarity deformations.

Figure 13 presents the fission barrier for fermium isotopes in two cases: with $(\beta_2, \beta_3, \beta_4, \beta_5)$ deformations (solid lines) and when only β_2 and β_4 parameters are included (dashed lines). As it is seen when the reflection asymmetry is included, the barriers become shorter. The reduction of the barrier is very similar for each isotope.

Figure 14 shows the spontaneous fission half-lives for fermium isotopes calculated in the 4-dimensional $(\beta_2, \beta_3, \beta_4, \beta_5)$ and 2-dimensional (β_2, β_4) collective spaces. In the Figure the experimental data are denoted with full circles, T_{sf} obtained in 4-dimensional deformation space $(\beta_2, \beta_4, \beta_3, \beta_5)$ by

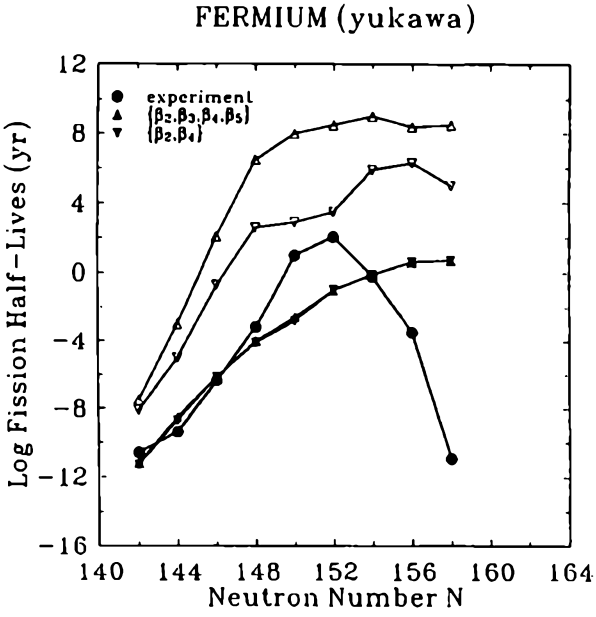

Fig. 14. The T_{sf} for the fermium isotopes in $(\beta_2, \beta_3, \beta_4, \beta_5)$ and (β_2, β_4) deformation spaces

Czasy życia T_{sf} dla izotopów fermu wyznaczone w przestrzeni kolektywnej $(\beta_2, \beta_3, \beta_4, \beta_5)$ i (β_2, β_4)

up-triangles and values obtained in 2-dimensional deformation space (β_2,β_4) with down-triangles. The full symbols denote the dynamical results, the open statical ones. From the Figure we can see that in the dynamical calculations the results in 4- and 2-dimensional space are practically the same. It is seen that the spontaneous fission process prefers the shapes of nuclei with $\beta_3 = \beta_5 = 0$. The above conclusion confirm Figure 15 where the paths to fission are shown in β_2 profile. It is seen that the dynamical paths β_3 and β_5 are the straight lines while the statical ones give values different from zero. From this investigations one can draw that odd-multipolarity deformations β_3 and β_5 do not play any role in the dynamical method of calculations of the T_{sf} in this region of nuclei.

In Figure 14 the statical values of T_{sf} are too large in comparison with the experiment. Moreover it is seen that the statical values of T_{sf} in 4-dimensional collective space lie about 2–4 orders of magnitude higher than the ones obtained in 2-dimensional space, despite the fact that statical fission barriers in 4-dimensional space are shorter. Generally speaking it is caused by "the longer valley to fission" in the more rich collective space.

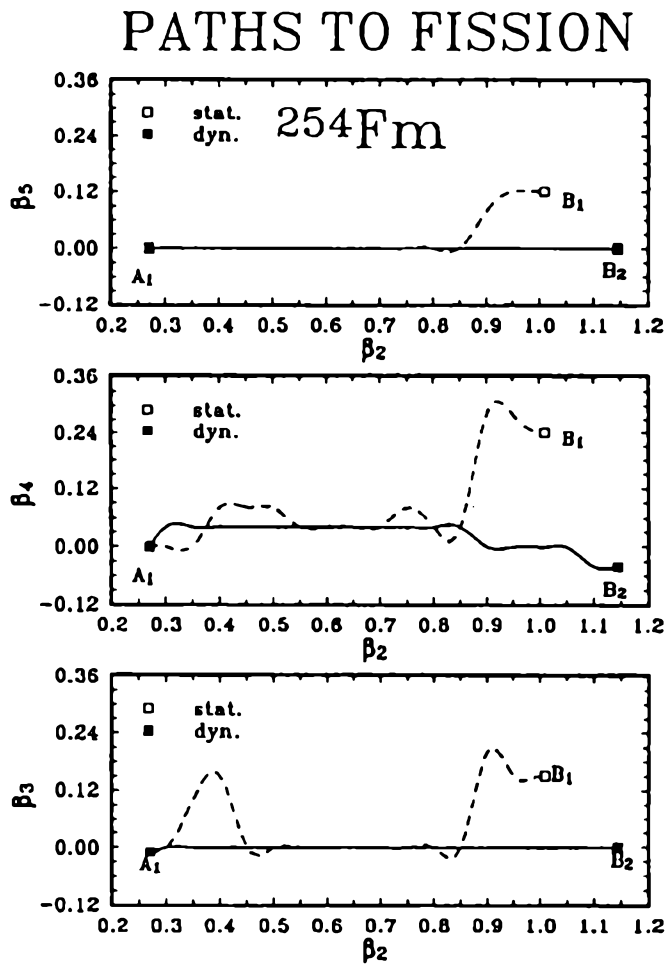

Fig. 15. The paths to fission in collective space $(\beta_2, \beta_3, \beta_4, \beta_5)$ for ^{254}Fm
Ścieżki do rozszczepienia uzyskane w przestrzeni kolektywnej $(\beta_2, \beta_3, \beta_4, \beta_5)$ dla ^{254}Fm

In order to study the influence of the even-parity of deformations of higher multipolarity on the T_{sf} we have performed the calculations in the deformation spaces of various dimensions. Figure 16 shows the theoretical values of T_{sf} calculated successively in the 4-dimensional deformation space $(\beta_2,\beta_4, \beta_6,\beta_8)$ (up-triangles), in 3-dimensional $(\beta_2,\beta_4,\beta_6)$ (down-triangles) and in the standard 2-dimensional (β_2,β_4) collective space (squares). The experimental data are denoted with full circles.

As previously, the open symbols denote the statical results, the full dynamical ones. One can see that only the deformation β_6 changes the dyna-

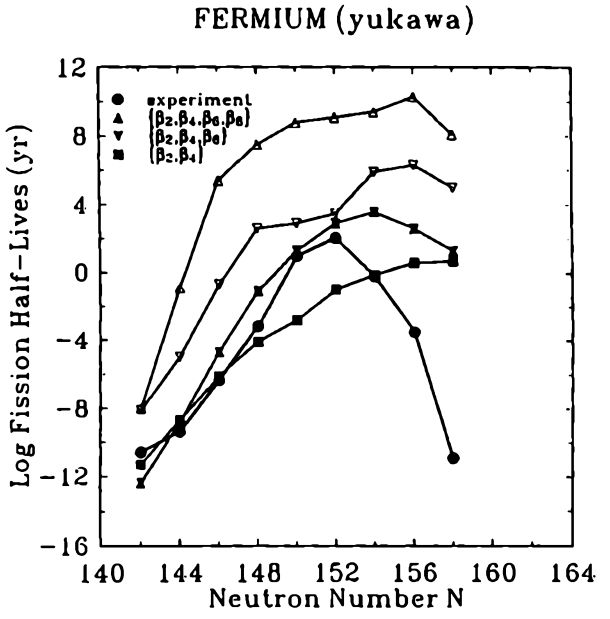

Fig. 16. The T_{sf} for the fermium isotopes in $(\beta_2,\beta_4,\beta_6,\beta_8)$, $(\beta_2,\beta_4,\beta_6)$ and (β_2,β_4) deformation spaces

Czasy życia T_{sf} izotopów fermu uzyskane w przestrzeni kolektywnej $(\beta_2,\beta_4,\beta_6,\beta_8)$, $(\beta_2,\beta_4,\beta_6)$ oraz (β_2,β_4)

mical results of the T_{sf} (the calculations with and without β_8 give almost the same results). The spontaneous fission half-lives with β_6 increase T_{sf} about 1–4 orders of magnitude. This effect improves a little the agreement with experiment, but for the nuclei with N $\geqslant$ 154 the difference between theory and experiment still reaches 4–6 orders of magnitude. We can conclude that only β_6 deformation, in addition to β_2 and β_4, is important in the dynamical calculations of the T_{sf}. In this case the statical results of T_{sf} in 4-dimensional collective space are larger about 1–5 orders of magnitude than the ones obtained in 3-dimensional space.

We are obliged to give some remarks about the statical method of the calculation of T_{sf}. From the above investigations of the spaces of various dimensions and various set of collective coordinates we can conclude that the statical results of the T_{sf} are strongly dependent on the dimension of the collective space. Especially it is well illustrated in the case of the odd-parity deformations (β_3 and β_5). Inclusion of these deformations leads to the considerable decrease of statical fission barriers for large deformations (see Figure 12), but after all the statical spontaneous fission half-lives becomes larger. It is caused, as we wrote above, by longer path to fission in the more

rich collective space. If in calculations of the T_{sf} we apply the "combined" [16] procedure e.g. the minimization of the potential energy in (β_3 and β_5) deformations and dynamical calculations in (β_2, β_4) space it leads to the reduction of the fission barrier and together with the shorter subbarrier trajectory in (β_2, β_4) space to considerable reduction of the spontaneous fission half-life. Hence it appears that the combined method in which the energy is minimized in selected degrees of freedom may leads to errors.

In order to describe properly the spontaneous fission half-lives of the heaviest nuclei we have to revise the parameters of the Woods-Saxon potential, especially the dependence of the spin-orbit part on deformations and if it is possible to expand the dynamical-programming method to five dimensions: $(\beta_2, \beta_4, \beta_6, \Delta_p, \Delta_n)$.

3. CONCLUSIONS

The following conclusions can be drawn from our investigations:

1. The investigations show that the pairing degrees of freedom are important in calculations of the spontaneous fission lifetimes.
2. The model with Woods-Saxon potential gives the T_{sf} on a good agreement with experimental data for the nuclei with atomic number $Z \geqslant 104$.
3. The calculations of T_{sf} show that it is very important to use the dynamic path to fission.
4. The lifetimes T_{sf} evaluated along the static trajectories are too large in comparison with experimental data and strongly dependent from dimension of collective spaces.
5. The theoretical estimates of T_{sf} are weakly dependent on the model used as macroscopic smooth part of the potential energy.
6. The odd-multipolarity deformations β_3 and β_5 do not play an important role in the theoretical calculations of the spontaneous fission half-lives.
7. For higher even-multipolarity deformations only β_6 is important in the calculations of the T_{sf}.
8. The calculations of T_{sf} with Woods-Saxon potential do not reproduce the experimentally known effect of the decrease of the fission lifetimes with the increase neutron number for $N \geqslant 152$ for fermium and nobelium isotopes.

ACKNOWLEDGMENT

We are thankful to Professor Krzysztof Pomorski and Dr Andrzej Baran for many valuable discussions, suggestions and comments.

Work supported partly by KBN, Project No. 2P 03B 049 09.

PACS numbers: 25.85.Ca;21.60.Ev;21.10.Tg.

REFERENCES

[1] Nilsson S. G., Tsang C. F., Sobiczewski A., Szymański, Z., Wycech S., Gustafson C., Lamm I. L., Möller P. and Nilsson B., *Nucl. Phys., A* 131 (1969) 1.

[2] Sobiczewski A., Szymański, Z., Wycech S., Nilsson S. G., Nix J. R., Tsang C. F., Gustafson C., Möller P. and Nilsson B., *Nucl. Phys., A* 131 (1969) 67.

[3] Randrup J., Tsang C. F., Möller P. and Nilsson S. G. *Nucl. Phys., A* 217 (1973) 221.

[4] Randrup J., Larsson S. E., Möller P., Nilsson S. G., Pomorski K. and Sobiczewski A., *Phys. Rev., C* 13 (1979) 229.

[5] Baran A., Łukasiak, A., Pomorski K. and Sobiczewski A., *Nucl. Phys., A* 361 (1981) 83.

[6] Baran A., *Phys. Lett.*, 76*B* (1978) 8.

[7] Baran A., Pomorski K., Larsson S. E., Möller P., Nilsson S. G., Randrup J., Łukasiak, A. and Sobiczewski A., *Proc. 4th IAEA Symp. on Physics and Chemistry of Fission*, Jülich 1979.

[8] Böning K., Patyk Z., Sobiczewski A. and Ćwiok S., *Z. Phys., A* 325 (1986) 479.

[9] Łojewski Z., Baran A., *Z. Phys., A* 329 (1988) 161.

[10] Dudek J., Werner T., *J. Phys., G* 4 (1978) 1543.

[11] Ćwiok S., Rozmej P., Sobiczewski A. and Patyk Z., *Nucl. Phys., A* 491 (1989) 281.

[12] Strutinsky V. M., *Nucl. Phys., A* 95 (1967) 420; *Nucl. Phys., A* 122 (1968) 1.

[13] Patyk Z., Sobiczewski A., *Nucl. Phys., A* 533 (1991) 132.

[14] Ćwiok S., Sobiczewski A., *Z. Phys., A* 342 (1992) 203.

[15] Ćwiok S., Hofmann S. and Nazarewicz W., *Nucl. Phys., A* 573 (1994) 356.

[16] Smolańczuk R., Skalski J. and Sobiczewski A., *Phys. Rev., C* 52 (19195) 1871.

[17] Staszczak A., Piłat S. and Pomorski K., *Nucl. Phys., A* 504 (1989) 589.

[18] Ćwiok S., Dudek J., Nazarewicz W., Skalski J. and Werner T., *Comp. Phys. Comm.*, 46 (1987) 379.

[19] Myers V., Świątecki W. J., *Ark. Fys.*, 36 (1967) 343.

[20] Krappe H. J., Nix J. R. and Sierk A. J., *Phys. Rev., C* 20 (1979) 992.

[21] Möller P., Nix R. J. and Świątecki W. J., *Nucl. Phys., A* 469 (1987) 1.

[22] Dudek J., Majhofer A. and Skalski J., *J. Phys., G* 6 (1980) 447.

[23] Góźdź A., Pomorski K., *Nucl. Phys., A* 451 (1986) 1.

STRESZCZENIE

W artykule prezentowane są wyniki badań dotyczących czasów połowicznego zaniku T_{sf} w procesie spontanicznego rozszczepienia parzyto-parzystych jąder atomowych o liczbach masowych $A = 100 \div 110$.

Do obliczeń czasów życia T_{sf} wykorzystano półklasyczne przybliżenie WKB. Bariery na rozszczepienie wyznaczono w modelu mikroskopowo-makroskopowym z użyciem jednocząstkowego potencjału typu Woodsa-Saxona, natomiast parametry masowe w przybliżeniu adiabatycznym "cranking". Klasyczne trajektorie prowadzące do rozszczepienia poszukiwane były w czterowymiarowej przestrzeni parametrów kolektywnych $(\beta_2, \beta_4, \Delta_p, \Delta_n)$. Dwa pierwsze parametry β_2 i β_4 opisują deformację kształtu jądra atomowego, a pozostałe Δ_p i Δ_n związane są z tzw. oddziaływaniem resztkowym "pairing".

Prezentowane czasy życia T_{sf} wyznaczano w sposób w pełni dynamiczny z uwzględnieniem zarówno efektów pochodzących od barier potencjału, jak i parametrów masowych.